

# The impact of the quantized transverse motion on radiation emission in a Dirac harmonic oscillator

Tobias N. Wistisen and Antonino Di Piazza

*Max-Planck-Institut für Kernphysik, Saupfercheckweg 1, D-69117, Germany*

We investigate the radiation emitted by an ultrarelativistic electron traveling in a 1-dimensional parabolic potential. Having in mind a simplified model for beamstrahlung, we consider the realistic case of the electron motion being highly directional, with the transverse momentum being much smaller than the longitudinal one. In this case we can find solutions of the Dirac equation and we calculate exactly the radiation emission using first-order perturbation theory. We compare the results obtained to that obtained via the semi-classical method of Baier and Katkov which includes quantum effects due to photon recoil in the radiation emission but ignores the quantum nature of the electron motion. On the one hand, we confirm a prediction of the semi-classical method that the emission spectrum should coincide with that in the case of a linearly polarized monochromatic wave. On the other hand, however, we find that the semi-classical method does not yield the exact result when the quantum number describing the transverse motion becomes small. In this way, we address quantitatively the problem of the limits of validity of the semi-classical method, which is known, generally speaking, to be applicable for large quantum numbers. Finally, we also discuss which beam conditions would be necessary to enter the studied regime where also the motion of the particles must be considered quantum mechanically to yield the correct spectrum.

## I. INTRODUCTION

Strong-field QED is the study of electromagnetic phenomena in the presence of background electromagnetic fields, whose strength approaches a critical limit, called the “Schwinger limit” [1–5]. In this limit phenomena that are of a purely quantum mechanical nature arise, such as pair production and vacuum birefringence [6, 7, 7–25], and quantum effects in radiation emission become essential [2, 12, 26–35, 35–49]. Most of the mentioned studies consider a plane-wave as a background field, having in mind processes occurring in the presence of a strong laser field. In this respect, there is also a growing interest in finding out how the basic strong-field QED processes mentioned above are altered in the presence of a laser beams tightly focused in space other than in time [48, 50–55]. In this paper, however, our focus is not on laser fields, but on different methods of calculating radiation emission, in particular a comparison between a fully quantum calculation compared to a semi-classical method, which can also be used for the case of lasers [7].

The semi-classical operator method developed by Baier and Katkov in 1968 [56] is a powerful method to calculate radiation emission and the probabilities of other quantum processes. Quantum effects such as spin and recoil during emission are included in the method but the motion of the charged particle is considered as classical, i.e., along a trajectory. Thus, in order to calculate the quantum observables, only the particle’s trajectory is needed, which can be found numerically in an arbitrary field configuration. Using this method to calculate nonlinear Compton scattering in more complex field configurations was the focus of [46]. Now, finding the wave-function of an electron in any given field configuration is in general an impossible task and it is therefore prudent to ask exactly when the method of Baier and Katkov is applicable. This is of course discussed by the authors themselves

and the mentioned conditions are that the particle should be ultra-relativistic and that the commutator among the operators corresponding to different velocity components should be negligibly small, in the sense that [26]

$$\frac{\left| \langle [\hat{\Pi}^\mu, \hat{\Pi}^\nu] \rangle \right|}{\varepsilon^2} = \frac{e |F^{\mu\nu}(x)|}{\varepsilon^2} \ll 1, \quad (1)$$

where  $\hat{\Pi}^\mu = \hat{p}^\mu + eA^\mu(x)$ ,  $\hat{p}^\mu$  is the four-momentum operator,  $e > 0$  is the elementary charge,  $A^\mu(x) = (\varphi(x), \mathbf{A}(x))$  is the four-vector potential of the external field,  $F^{\mu\nu}(x)$  is the electromagnetic field tensor and  $\varepsilon$  is the particle energy. This condition is, indeed, fulfilled for any currently imaginable electromagnetic field. For the well-known exact solutions of the Dirac equation in the field configurations of a plane wave [2], the semi-classical operator method yields exactly the same result as the full quantum calculation. In the final step of the derivation of the method in [56], it is stated that since the unfolding of a certain operator has been performed, the expectation value of this operator can be replaced by its corresponding classical value. This, however, may not always be allowed, even when the previously mentioned conditions are fulfilled. The field configuration studied in the present paper is an example of this. In the book [26] by the same authors, an additional condition has been added, that one can replace the expectation value of the operator with the classical value when the quantum state of the electron is characterized by large quantum numbers. This is in line with Bohr’s correspondence principle. In the present paper we investigate exactly this aspect of the method of Baier and Katkov: the method reproduces the correct quantum result when the quantum numbers describing the motion are large. In [26] the semi-classical method has, naturally, also been employed to study the radiation from the relativistic harmonic oscillator, which is in essence the problem studied here.

In this paper we also include a magnetic field such that the field also can be employed as a simplified model of “beamstrahlung”, i.e. the radiation emitted when high-energy dense charged bunches collide. In our solution we can turn off the magnetic field component and thus also obtain the results of the harmonic oscillator as in [26]. In fact, the only effect of the magnetic field is to effectively make the oscillator twice as strong. Usually, in future linear colliders, the colliding bunches are of identical shape and oppositely charged, i.e. an electron bunch colliding with a positron bunch. In this case during the collision, the field from one bunch will alter the shape of the other bunch and vice versa. The full problem is therefore multi-particle, making it complicated to fully solve it quantum mechanically. However the classical motion can be solved in this case, and therefore the semi-classical method of Baier and Katkov can be applied. In this paper, however, the main interest is not to make a precise analysis of beamstrahlung, but to investigate when and why the semi-classical approach breaks down. We therefore consider the case where a single electron interacts with the field of a positron bunch as in this way the positron bunch can be assumed not to change shape during the collision. This solution would still be valid if one studies the collision of a low-density bunch with a high-density bunch, such that the low-density bunch has only negligible effect on the dense one.

As shown in [26], the result of the semi-classical operator method applied to the one-dimensional oscillator problem yields simply the spectrum obtained in the case of nonlinear Compton scattering in a linearly polarized monochromatic plane wave as found in, e.g., [2]. As we shall see, the correct calculation will deviate from this result when the quantum number of the discretized transverse motion becomes small. However, since this comparison is an important point, below we will also apply the semi-classical operator method to this problem [26]. In section §II we will first make some considerations on the electromagnetic field generated from the relativistic positron bunch and indicate how one arrives at the parabolic potential approximation. In section §III we will gain an intuition of the problem and find an approximated analytical solution of the classical equations of motion of the problem, enabling us to apply the semi-classical method of Baier and Katkov in section §VI. In section §IV we find the approximate wave-functions for the problem at hand and in section §V we use these wave-functions to calculate the transition matrix element of the single-photon radiation emission. In section §VII we do a side-by-side comparison of the power spectra obtained using the two methods of calculation and discuss the different regimes of radiation emission which arise. Finally in section §VIII we draw the main conclusions of the paper.

We use units where  $\hbar = c = 1$ ,  $\alpha = e^2$  and the Feynman slash notation such that  $\not{a} = a_\mu \gamma^\mu$ , where  $\gamma^\mu$  are the Dirac gamma matrices and  $a^\mu$  an arbitrary four-vector. We adopt the metric tensor  $\eta^{\mu\nu} = \text{diag}(+1, -1, -1, -1)$ .

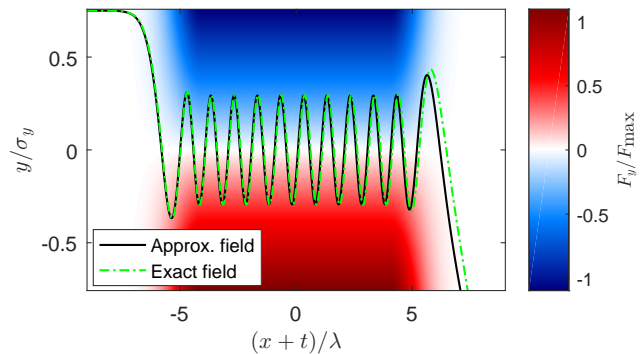


Figure 1: The  $y$ -component  $F_y$  of the force exerted by a positron bunch propagating along the positive  $x$ -direction and lying on the  $x$ - $z$  plane as function of position and time. Here,  $F_{\max}$  is the magnitude of the force at  $x + t = 0$  and  $y/\Sigma_y = 0.75$ ,  $\lambda = 2\pi/\omega_0$  [see Eq. (26)]. The black continuous line corresponds to the electron’s trajectory using a Gaussian distribution for the charge density of the bunch [57, 58], whereas the green dashed-dotted line corresponds to the approximated model described in the text [see equation (3)].

## II. MODEL OF THE FIELD

Let us now consider a model of the electromagnetic field from the dense positron bunch. The bunches to be used in linear colliders are usually shaped like sheets, that is they are much longer than they are wide, and much thinner than they are wide. By assuming that the bunch propagates along the positive  $x$  direction and it lies on the  $x$ - $z$  plane, the r.m.s. values of the charge distribution in space are such that  $\Sigma_y \ll \Sigma_z \ll \Sigma_x$  (see figure 1). We first consider the field in the co-moving frame of the bunch. Here, the transverse beam sizes  $\Sigma_y$  and  $\Sigma_z$  remain unchanged, while the longitudinal becomes longer by a factor of  $\gamma_b$ , which is the Lorentz factor of the bunch, due to the effect of Lorentz contraction. Therefore in this co-moving frame the bunches are still sheets. The charge density is often modeled as a Gaussian function, that is

$$\rho'(\mathbf{r}') = \frac{Ne}{(2\pi)^{3/2}\Sigma'_x\Sigma'_y\Sigma'_z} e^{-\left(\frac{x'^2}{2\Sigma_x'^2} + \frac{y'^2}{2\Sigma_y'^2} + \frac{z'^2}{2\Sigma_z'^2}\right)}, \quad (2)$$

where primed quantities refer to quantities in the co-moving frame and  $N$  the number of positrons in the bunch. To obtain the electric field one can use Gauss’ law,  $\nabla' \cdot \mathbf{E}'(\mathbf{r}') = 4\pi\rho'(\mathbf{r}')$ , as explained in [57, 58]. However, since the bunches are flat, there will be a large component of the field only orthogonal to the sheet, i.e., along the  $y'$  (or  $y$ ) direction. Moreover, imagining to describe processes occurring at the center of the bunch, we can make the leading order expansion of the field component, which results in

$$E'_{y'}(\mathbf{r}') \simeq \frac{4\pi Ne}{(2\pi)^{3/2}\Sigma'_x\Sigma'_y\Sigma'_z} y'. \quad (3)$$

To obtain the field in the lab-frame we perform a Lorentz transformation with velocity given by  $-\beta_b$ , with  $\beta_b$  being the velocity of the bunch. The orthogonal component of the electric field becomes boosted by a factor of the bunch Lorentz factor  $\gamma_b$ , which simplifies with the corresponding change in the bunch length  $\Sigma'_z = \gamma_b \Sigma_z$  and one obtains

$$E_y(\mathbf{r}) = \frac{4\pi N e}{(2\pi)^{3/2} \Sigma_x \Sigma_y \Sigma_z} y. \quad (4)$$

A magnetic field arises according to the Lorentz transformation of the electromagnetic fields:

$$\mathbf{B}_\perp(\mathbf{r}) = -\gamma_b \beta_b \times \mathbf{E}'(\mathbf{r}') = -\beta_b E_y(\mathbf{r}) \mathbf{e}_3, \quad (5)$$

where  $\mathbf{e}_3$  is a unit vector in the  $z$  direction. In order to neglect the dependence of the fields on  $x$  and  $t$ , we have implicitly assumed that the electron moves along the  $x$  direction at a speed close to the speed of light like the bunch and that the dynamics in the  $y$  direction occurs on a timescale much shorter than  $\Sigma_x$ . For the parameters chosen in figure 1, for example, one can see that our approximations result in a trajectory very close to the exact one. Due to the fact that in a number of situations one can approximate an electromagnetic field as a linear function of a coordinate, this model is still useful not only as a toy model for beamstrahlung but also to identify the new regime where the transverse motion must be treated quantum mechanically, instead of classically. In conclusion, the only non-zero components of the background electromagnetic field in the laboratory frame are given by

$$E_y(\mathbf{r}) = \kappa y, \quad (6)$$

$$B_z(\mathbf{r}) = -\beta_b \kappa y, \quad (7)$$

where

$$\kappa = \frac{2Ne}{\sqrt{2\pi} \Sigma_x \Sigma_y \Sigma_z}, \quad (8)$$

is the field gradient.

### III. CLASSICAL MOTION

To gain a basic understanding of the problem at hand we first consider the classical motion in the given field configuration. We are interested in the case of an ultrarelativistic electron with the motion being mainly directed along the positive  $x$ -axis, i.e. the  $x$  component of the velocity  $\mathbf{v}$  fulfills the condition  $v_x \simeq 1$ , whereas the transverse momentum is much smaller than the longitudinal one. In particular, we assume that the the initial time is set equal to zero and that  $v_z(0) = 0$ , in such a way that  $v_z(t) = 0$  for all  $t > 0$ . Since the transverse motion is only along the  $y$  direction, it is convenient to introduce the parameter

$$\xi = \gamma_0 v_{y,\max}, \quad (9)$$

where  $\gamma_0$  is the initial electron Lorentz gamma factor. The parameter  $\xi$  then becomes on the order of unity when the transverse motion becomes relativistic. We will restrict ourselves to the (broad) case where  $v_{y,\max} \ll 1$  and therefore  $\xi \ll \gamma_0$ . The two conditions  $v_x \simeq 1$  and  $\xi \ll \gamma_0$  will be employed below to solve the equations of motion. We use the Lorentz force equation, with the electric and magnetic force terms given by

$$q\mathbf{E} = \begin{pmatrix} 0 \\ -e\kappa y \\ 0 \end{pmatrix}, \quad (10)$$

and

$$\begin{aligned} q\mathbf{v} \times \mathbf{B} &= (-e) \begin{pmatrix} v_x \\ v_y \\ v_z \end{pmatrix} \times \begin{pmatrix} 0 \\ 0 \\ 1 \end{pmatrix} (-\kappa\beta_b y) \\ &= \beta_b e\kappa y \begin{pmatrix} v_y \\ -v_x \\ 0 \end{pmatrix}, \end{aligned} \quad (11)$$

respectively. The non-vanishing components of the Lorentz equation read

$$\frac{dp_x}{dt} = \beta_b e\kappa y v_y, \quad (12)$$

$$\frac{dp_y}{dt} = -e\kappa y - e\beta_b \kappa y v_x = -(1 + \beta_b v_x) e\kappa y. \quad (13)$$

Now we use the identity

$$\frac{d\mathbf{p}}{dt} = \frac{d\gamma}{dt} m\mathbf{v} + \gamma m \frac{d\mathbf{v}}{dt}, \quad (14)$$

where  $m$  is the electron mass. By using the equation for the variation of the energy

$$m \frac{d\gamma}{dt} = q\mathbf{E} \cdot \mathbf{v} = -e\kappa y v_y, \quad (15)$$

we obtain

$$\begin{aligned} \gamma m \frac{dv_x}{dt} &= q(\mathbf{E} + \mathbf{v} \times \mathbf{B})_x - \frac{d\gamma}{dt} m v_x \\ &= (\beta_b e\kappa y v_y) - (-e\kappa y v_y) v_x \\ &= (v_x + \beta_b) e\kappa y v_y, \end{aligned} \quad (16)$$

and

$$\begin{aligned} \gamma m \frac{dv_y}{dt} &= q(\mathbf{E} + \mathbf{v} \times \mathbf{B})_y - \frac{d\gamma}{dt} m v_y \\ &= -e\kappa y - \beta_b e\kappa y v_x - (-e\kappa y v_y) v_y \\ &= -e\kappa y (1 + \beta_b v_x - v_y^2). \end{aligned} \quad (17)$$

Now we write

$$v_x(t) = 1 + \delta v_x(t), \quad (18)$$

and

$$\gamma(t) = \gamma_0 + \delta\gamma(t), \quad (19)$$

where  $\gamma_0$  is the initial value of the Lorentz gamma factor for the electron. So we obtain the exact equations of motion as

$$\frac{d\delta v_x}{dt} = \frac{1}{\gamma_0} \frac{1}{1 + \frac{\delta\gamma}{\gamma_0}} (\beta_b + 1 + \delta v_x) \frac{e\kappa}{m} y v_y, \quad (20)$$

$$\frac{dv_y}{dt} = -\frac{1}{\gamma_0} \frac{1}{1 + \frac{\delta\gamma}{\gamma_0}} (1 + \beta_b + \beta_b \delta v_x - v_y^2) \frac{e\kappa}{m} y. \quad (21)$$

Now we wish to find solutions under the conditions  $v_y^2(t) \ll 1$ ,  $|\delta v_x(t)| \ll 1$ ,  $|\delta\gamma(t)| \ll \gamma_0$  and  $1/\gamma_b^2 \ll 1$ . In this case the equations simplify significantly and we will verify that the obtained solutions verify these conditions. The approximate equations of motion then become

$$\frac{d\delta v_x}{dt} = (1 + \beta_b) \frac{e\kappa}{\gamma_0 m} y v_y, \quad (22)$$

$$\frac{dv_y}{dt} = -(1 + \beta_b) \frac{e\kappa}{\gamma_0 m} y. \quad (23)$$

Here, one can replace  $\beta_b$  by unity but we prefer to keep the symbol  $\beta_b$  such that we can obtain the case of a harmonic oscillator via the replacement  $\beta_b = 0$ . Now the equation for  $y$  can be solved with appropriate initial conditions to obtain

$$v_y(t) = \frac{\xi}{\gamma_0} \cos(\omega_0 t), \quad (24)$$

$$y(t) = y_{\max} \sin(\omega_0 t), \quad (25)$$

where

$$\omega_0 = \sqrt{\frac{(1 + \beta_b) e\kappa}{\gamma_0 m}}. \quad (26)$$

And from the definition of Eq. (9) we obtain that the amplitude can be expressed in terms of the previously defined quantities as

$$y_{\max} = \frac{\xi}{\gamma_0 \omega_0}. \quad (27)$$

Now we can solve the equation for the motion along the  $x$  direction.

$$\begin{aligned} \frac{d\delta v_x}{dt} &= \omega_0^2 y v_y \\ &= \omega_0 \left( \frac{\xi}{\gamma_0} \right)^2 \sin(\omega_0 t) \cos(\omega_0 t) \\ &= \frac{\omega_0}{2} \left( \frac{\xi}{\gamma_0} \right)^2 \sin(2\omega_0 t), \end{aligned} \quad (28)$$

and upon integration we obtain

$$\delta v_x(t) = -\frac{1}{4} \left( \frac{\xi}{\gamma_0} \right)^2 \cos(2\omega_0 t) + C_1, \quad (29)$$

where  $C_1$  is a constant of integration. Now, the constant difference between  $\delta v_x(t)$  and  $v_x(t)$  can be absorbed in the constant of integration  $C_1$  in Eq. (29) such that

$$v_x(t) = -\frac{1}{4} \left( \frac{\xi}{\gamma_0} \right)^2 \cos(2\omega_0 t) + C_2. \quad (30)$$

In order to determine the constant  $C_2$ , we can use  $v_x^2(0) + v_y^2(0) = v_0^2 = 1 - 1/\gamma_0^2$ . Thus,  $v_x^2(0) = 1 - (1 + \xi^2)/\gamma_0^2$  and  $v_x(0) \simeq 1 - (1 + \xi^2)/2\gamma_0^2$ , we can determine the constant of integration  $C_2$  and we obtain:

$$v_x(t) = 1 - \frac{1}{2\gamma_0^2} - \frac{\xi^2}{4\gamma_0^2} - \frac{\xi^2}{4\gamma_0^2} \cos(2\omega_0 t), \quad (31)$$

which upon integration yields

$$x(t) = \left( 1 - \frac{1}{2\gamma_0^2} - \frac{\xi^2}{4\gamma_0^2} \right) t - \frac{\xi^2}{4\gamma_0^2} \frac{\sin(2\omega_0 t)}{2\omega_0}. \quad (32)$$

Now, it is clear that the conditions for the approximate solutions are fulfilled as long as  $\xi \ll \gamma_0$ . However we must use Eq. (15) to check when the condition  $|\delta\gamma(t)| \ll \gamma_0$  is fulfilled. Using Eq. (15) we obtain

$$\frac{d\gamma}{dt} = -\frac{\omega_0}{1 + \beta_b} \frac{\xi^2}{2\gamma_0} \sin(2\omega_0 t). \quad (33)$$

And so we can integrate to obtain

$$\gamma(t) = \gamma_0 + \frac{1}{1 + \beta_b} \frac{\xi^2}{4\gamma_0} [\cos(2\omega_0 t) - 1], \quad (34)$$

and therefore

$$\frac{\delta\gamma(t)}{\gamma_0} = \frac{1}{1 + \beta_b} \frac{\xi^2}{4\gamma_0^2} [\cos(2\omega_0 t) - 1]. \quad (35)$$

In this way the condition  $|\delta\gamma(t)| \ll \gamma_0$  is equivalent to the condition  $\xi \ll \gamma_0$ . Therefore, as long as this condition is fulfilled the neglected terms are smaller than a factor of at least  $\xi/\gamma_0$  compared to the dominant ones.

#### IV. SOLUTION OF DIRAC EQUATION

Classically the fields of Eq. (6) and (7) gives a force as in Hooke's law and therefore harmonic oscillations as seen in section (III). Harmonic oscillator wave functions should therefore be involved in the solution of the Dirac equation. We have  $\mathbf{E}(\mathbf{r}) = -\nabla\varphi(\mathbf{r})$  so due to the simple structure of the electric field in Eq. (6) the potential depends only on the  $y$ -coordinate, i.e. we have

$$\varphi(y) = -\frac{\kappa y^2}{2}. \quad (36)$$

A vector potential which gives us the magnetic field of Eq. (7) is

$$\mathbf{A}(y) = \frac{\beta_b \kappa}{2} (y^2, 0, 0). \quad (37)$$

The Dirac equation in an external field reads

$$(\hat{\mathbf{p}} + e\mathbf{A}(\mathbf{r}) - m) \psi(\mathbf{r}, t) = 0, \quad (38)$$

where  $\psi(\mathbf{r}, t)$  is the electron bispinor wave function. This can also be rewritten as

$$i \frac{\partial \psi(\mathbf{r}, t)}{\partial t} = \hat{H} \psi(\mathbf{r}, t), \quad (39)$$

with

$$\hat{H} = \boldsymbol{\alpha} \cdot \hat{\boldsymbol{\Pi}} - e\varphi(\mathbf{r}) + \gamma^0 m, \quad (40)$$

where  $\boldsymbol{\alpha}^i = \gamma^0 \gamma^i$ ,  $i = 1, 2, 3$ , and  $\boldsymbol{\Pi}_i = \hat{\mathbf{p}}_i + e\mathbf{A}_i(\mathbf{r})$  (for electron). We consider a problem where the potentials have no time dependence and then take the usual approach [59] of finding the stationary states and write

$$\psi(\mathbf{r}, t) = e^{-i\varepsilon t} \begin{pmatrix} \phi(\mathbf{r}) \\ \chi(\mathbf{r}) \end{pmatrix}, \quad (41)$$

where  $\varepsilon$  will be the energy. This leads to

$$(\varepsilon - V(\mathbf{r}) - m)\phi(\mathbf{r}) = \boldsymbol{\sigma} \cdot (-i\nabla + e\mathbf{A}(\mathbf{r}))\chi(\mathbf{r}), \quad (42)$$

$$(\varepsilon - V(\mathbf{r}) + m)\chi(\mathbf{r}) = \boldsymbol{\sigma} \cdot (-i\nabla + e\mathbf{A}(\mathbf{r}))\phi(\mathbf{r}), \quad (43)$$

where  $\boldsymbol{\sigma}$  denote the three Pauli matrices. Now from Eq. (42) we find

$$\chi(\mathbf{r}) = \frac{1}{\varepsilon + e\varphi(y) + m} \boldsymbol{\sigma} \cdot \hat{\boldsymbol{\Pi}} \phi(\mathbf{r}), \quad (44)$$

and inserting this in Eq. (43) we obtain a differential equation for  $\phi(\mathbf{r})$

$$\begin{aligned} & (\varepsilon + e\varphi(y) - m)\phi(\mathbf{r}) \\ &= \boldsymbol{\sigma} \cdot (-i\nabla + e\mathbf{A}(y)) \frac{1}{\varepsilon + e\varphi(y) + m} \boldsymbol{\sigma} \cdot \hat{\boldsymbol{\Pi}} \phi(\mathbf{r}). \end{aligned} \quad (45)$$

To find the solution for  $\phi(\mathbf{r})$  we need to rewrite this such that we can isolate the Laplacian of  $\phi(\mathbf{r})$ . The product rule for the gradient gives us a term where it acts on  $(\varepsilon + e\varphi(y) + m)^{-1}$  and one where it acts on  $\boldsymbol{\sigma} \cdot \hat{\boldsymbol{\Pi}} \phi(\mathbf{r})$  so this gives us

$$\begin{aligned} & (\varepsilon + e\varphi(y) - m)\phi(\mathbf{r}) \\ &= -i\boldsymbol{\sigma} \cdot \nabla \left( \frac{1}{\varepsilon + e\varphi(y) + m} \right) \boldsymbol{\sigma} \cdot \hat{\boldsymbol{\Pi}} \phi(\mathbf{r}) \\ &\quad - \frac{1}{\varepsilon + e\varphi(y) + m} i\boldsymbol{\sigma} \cdot \nabla \left( \boldsymbol{\sigma} \cdot \hat{\boldsymbol{\Pi}} \phi(\mathbf{r}) \right) \\ &\quad + \boldsymbol{\sigma} \cdot e\mathbf{A}(y) \frac{1}{\varepsilon + e\varphi(y) + m} \boldsymbol{\sigma} \cdot \hat{\boldsymbol{\Pi}} \phi(\mathbf{r}) \\ &= -i\boldsymbol{\sigma} \cdot \nabla \left( \frac{1}{\varepsilon + e\varphi(y) + m} \right) \boldsymbol{\sigma} \cdot \hat{\boldsymbol{\Pi}} \phi(\mathbf{r}) \\ &\quad + \frac{1}{\varepsilon + e\varphi(y) + m} \boldsymbol{\sigma} \cdot (-i\nabla + e\mathbf{A}(y)) \boldsymbol{\sigma} \cdot \hat{\boldsymbol{\Pi}} \phi(\mathbf{r}) \quad (46) \\ &= -i\boldsymbol{\sigma} \cdot \nabla \left( \frac{1}{\varepsilon + e\varphi(y) + m} \right) \boldsymbol{\sigma} \cdot \hat{\boldsymbol{\Pi}} \phi(\mathbf{r}) \\ &\quad + \frac{1}{\varepsilon + e\varphi(y) + m} \left[ \boldsymbol{\sigma} \cdot \hat{\boldsymbol{\Pi}} \right]^2 \phi(\mathbf{r}) \\ &= i\boldsymbol{\sigma}_y \cdot \frac{e\varphi'(y)}{(\varepsilon + e\varphi(y) + m)^2} \boldsymbol{\sigma} \cdot \hat{\boldsymbol{\Pi}} \phi(\mathbf{r}) \\ &\quad + \frac{1}{\varepsilon + e\varphi(y) + m} \left[ \boldsymbol{\sigma} \cdot \hat{\boldsymbol{\Pi}} \right]^2 \phi(\mathbf{r}). \end{aligned}$$

Multiplying by  $(\varepsilon + e\varphi(y) + m)$  on both sides we obtain

$$\begin{aligned} & ((\varepsilon + e\varphi(y))^2 - m^2) \phi(\mathbf{r}) \\ &= i\boldsymbol{\sigma}_y \cdot \frac{1}{\varepsilon + e\varphi(y) + m} e\varphi'(y) \boldsymbol{\sigma} \cdot \hat{\boldsymbol{\Pi}} \phi(\mathbf{r}) + \left[ \boldsymbol{\sigma} \cdot \hat{\boldsymbol{\Pi}} \right]^2 \phi(\mathbf{r}) \\ &= -i \frac{1}{\varepsilon + e\varphi(y) + m} (\boldsymbol{\sigma}_y \cdot eE_y(y)) \boldsymbol{\sigma} \cdot \hat{\boldsymbol{\Pi}} \phi(\mathbf{r}) + \left[ \boldsymbol{\sigma} \cdot \hat{\boldsymbol{\Pi}} \right]^2 \phi(\mathbf{r}) \\ &= \frac{-i}{\varepsilon + e\varphi(y) + m} \left( eE_y(y) \hat{\Pi}_y + i\boldsymbol{\sigma} \cdot (e\mathbf{E}(y) \times \hat{\boldsymbol{\Pi}}) \right) \phi(\mathbf{r}) \\ &\quad + \left[ \boldsymbol{\sigma} \cdot \hat{\boldsymbol{\Pi}} \right]^2 \phi(\mathbf{r}). \end{aligned} \quad (47)$$

Now we need to consider the term  $\left[ \boldsymbol{\sigma} \cdot \hat{\boldsymbol{\Pi}} \right]^2$  by letting it act on a test function  $f$ .

$$\begin{aligned} & [\boldsymbol{\sigma} \cdot (\hat{\mathbf{p}} + e\mathbf{A}(y))] [\boldsymbol{\sigma} \cdot (\hat{\mathbf{p}} f + e\mathbf{A}(y) f)] \\ &= \hat{\mathbf{p}}^2 f + \boldsymbol{\sigma} \cdot (\nabla \times [e\mathbf{A}(y)]) f \\ &\quad + 2eA_x(y) \hat{p}_x f + e^2 A^2(y) f. \end{aligned} \quad (48)$$

Then, finally, we obtain

$$\begin{aligned} & [\hat{\mathbf{p}}^2 + e\boldsymbol{\sigma} \cdot \mathbf{B}(y) + 2eA_x(y) \hat{p}_x \\ &\quad - 2\varepsilon e\varphi(y) + e^2 A^2(y) - e^2 \varphi^2(y) \\ &\quad - i \frac{1}{\varepsilon + e\varphi(y) + m} \left( eE_y \hat{\Pi}_y + i\boldsymbol{\sigma} \cdot (e\mathbf{E}(y) \times \hat{\boldsymbol{\Pi}}) \right) \\ &\quad - (\varepsilon^2 - m^2)] \phi(\mathbf{r}) = 0. \end{aligned} \quad (49)$$

This is the exact differential equation for  $\phi(\mathbf{r})$ . In Eq. (49) the dominant terms driving the dynamics are the terms  $2eA_x(y)\hat{p}_x - 2\varepsilon e\varphi(y)$ . We will try with a separable solution which yields free motion in the  $x$ -direction such that this becomes  $2eA_x(y)p_x$  (no longer an operator) which is under most circumstances nearly equal the other term  $-2\varepsilon e\varphi(y)$ . These two terms correspond to the adding of the electric and magnetic forces on the particle. It turns out that in the regime we are interested in, many of the terms in Eq. (49) can be neglected.

### A. $e^2\varphi^2(y)$ term

If  $e^2\varphi^2(y)$  should be much smaller than  $-2\varepsilon e\varphi(y)$  we should have that  $2\varepsilon \gg -e\varphi(y)$ . The most stringent condition is then to use  $-e\varphi_{\max} = -e\varphi(y_{\max}) = e\kappa y_{\max}^2/2 = e\kappa\xi^2/2\gamma_0^2\omega_0^2$ . Our condition then becomes  $1 \gg \frac{\xi^2}{\gamma_0^2} \frac{1}{4(1+\beta_b)}$ , a condition which will be fulfilled as we require exactly that  $\xi \ll \gamma_0$ . The same argument goes for the  $e^2A^2(y)$  term.

### B. $e\boldsymbol{\sigma} \cdot \mathbf{B}(y)$ term

Here we should have  $-2\varepsilon e\varphi(y) \gg eB_z(y)$  corresponding to

$$2\varepsilon \frac{e\kappa y^2}{2} \gg e\kappa y, \quad (50)$$

which reduces to

$$y \gg \frac{1}{\varepsilon}, \quad (51)$$

which is seen to be roughly the Compton wavelength divided by a factor of  $\gamma_0$ . The problem could, in fact, be solved while including this term, and the effect would be that the spin up and spin down wave-functions are shifted by the distance  $1/\varepsilon$  compared to each other. This is however completely negligible. As we will see later, the transition to the new regime happens when the typical length of the problem becomes on the order of the Compton wavelength, and this condition is a factor of  $\gamma_0$  below this.

### C. $\frac{eE_y\hat{\Pi}_y}{\varepsilon+e\varphi(y)+m}$ term

We obtain the most stringent condition by inserting the maximum value of the classical momentum and so

$$\frac{eE_y\hat{\Pi}_y}{\varepsilon+e\varphi(y)+m} \simeq \frac{e\kappa y p_{y,\max}}{\varepsilon} \simeq \frac{e\kappa y m \xi}{\varepsilon}. \quad (52)$$

We should then have

$$\frac{e\kappa y m \xi}{\varepsilon} \ll -2\varepsilon e\varphi(y) = \varepsilon e\kappa y^2, \quad (53)$$

which reduces to

$$y \gg \frac{\xi}{\gamma_0} \frac{1}{\varepsilon}, \quad (54)$$

and since we require that  $\gamma_0 \gg \xi$  if Eq. (51) is fulfilled, then so is Eq. (54).

### D. $\frac{\boldsymbol{\sigma} \cdot (e\mathbf{E} \times \hat{\boldsymbol{\Pi}})}{\varepsilon+e\varphi(y)+m}$

We have that  $\boldsymbol{\sigma} \cdot (\mathbf{E} \times \hat{\boldsymbol{\Pi}}) = \sigma_x E_y(y)p_z - \sigma_z E_y(y)(p_x + eA_x(y))$ . The previous terms have either had the matrix structure of the identity or  $\sigma_z$  while here we also have a term proportional to  $\sigma_x$  i.e. a mixing between the spin states. The  $\sigma_z$  term is on the same size as the one from section IV B and therefore negligible. The mixing term will be even smaller as  $p_z$  will be 0 initially and on the order of  $m$  in the final state, so a factor of  $\gamma_0$  smaller than the already negligible small correction.

Now that we have argued for the smallness of the additional terms we are left with the equation

$$[\hat{\mathbf{p}}^2 + 2eA_x(y)\hat{p}_x - 2\varepsilon e\varphi(y) - (\varepsilon^2 - m^2)] \phi(\mathbf{r}) = 0. \quad (55)$$

This gives us

$$[-\nabla^2 + e\kappa\beta y^2(-i\partial_x) + \varepsilon e\kappa y^2 - (\varepsilon^2 - m^2)] \phi(\mathbf{r}) = 0. \quad (56)$$

To solve this equation we try the ansatz  $\phi(\mathbf{r}) = I(y)e^{ip_x x + ip_z z}$  where  $\mathbf{s}$  is any 2-component vector and so we obtain the following differential equation only in the  $y$ -coordinate,

$$\left[ -\frac{d^2}{dy^2} + e\kappa(\beta_b p_x + \varepsilon)y^2 - (\varepsilon^2 - p_x^2 - p_z^2 - m^2) \right] I(y) = 0. \quad (57)$$

By defining

$$\frac{1}{L} = \sqrt[4]{e\kappa(\beta_b p_x + \varepsilon)}, \quad (58)$$

and introducing the dimensionless variable,

$$\eta = y/L, \quad (59)$$

we obtain that

$$\left[ \frac{d^2}{d\eta^2} - \eta^2 + L^2 (\varepsilon^2 - p_x^2 - p_z^2 - m^2) \right] I(\eta) = 0, \quad (60)$$

and defining

$$a = L^2 (\varepsilon^2 - p_x^2 - p_z^2 - m^2), \quad (61)$$

equation (60) becomes

$$\left[ \frac{d^2}{d\eta^2} - \eta^2 + a \right] I(\eta) = 0, \quad (62)$$

which has normalizable solutions when  $a = 2n + 1$  with  $n$  integer (see e.g. [60, 61]), which we denote  $I_n(\eta)$ . And so the solutions to Eq. (55) are given by

$$\phi_n(\mathbf{r}) = e^{i(p_x x + p_z z)} I_n(\eta(y)) \mathbf{s}, \quad (63)$$

when the constants are related by

$$\varepsilon_n^2 = \frac{1}{L^2} (2n + 1) + p_x^2 + p_z^2 + m^2, \quad (64)$$

and the solutions can be written explicitly as

$$I_n(\eta) = N_n e^{-\eta^2/2} H_n(\eta), \quad (65)$$

where  $N_n$  is a normalization constant to be found and  $H_n(\eta)$  are the Hermite polynomials normalized such that  $\int_{-\infty}^{\infty} H_m(x) H_n(x) e^{-x^2} dx = \sqrt{\pi} 2^n n! \delta_{nm}$  where  $\delta_{nm}$  is the Kronecker delta function. We would like to normalize  $I_n(\eta)$  such that

$$\int |I_n(\eta)|^2 dy = 1, \quad (66)$$

which gives us that

$$N_n = \frac{1}{\sqrt{2^n L \sqrt{\pi} n!}}. \quad (67)$$

So we have our solutions to the Dirac equation as

$$\psi(\mathbf{r}, t) = \frac{1}{\sqrt{2L_x L_z}} \left( \begin{array}{c} I_n(\eta) \mathbf{s} \\ \frac{\boldsymbol{\sigma} \cdot (-i\boldsymbol{\nabla} + e\mathbf{A}(y))}{\varepsilon + e\varphi(y) + m} I_n(\eta) \mathbf{s} \end{array} \right) e^{i(p_x x + p_z z - \varepsilon_n t)}, \quad (68)$$

where  $L_x L_z$  is a normalization area in the  $xz$  plane (1 particle per area). To obtain a more explicit expression for the lower two components in the bispinor of Eq. (68) we insert the Pauli matrices to obtain

$$\begin{aligned} & \boldsymbol{\sigma} \cdot (-i\mathbf{e}_2 \frac{d}{dy} + e\mathbf{A}(y)) I_n(\eta) \\ &= y^2 I_n(\eta) \frac{e\kappa\beta_b}{2} \boldsymbol{\sigma}_x - i\boldsymbol{\sigma}_y \frac{dI_n(\eta)}{dy} \\ &= \left( \begin{array}{cc} 0 & I_n(\eta)\eta^2 C - \frac{1}{L} \frac{dI_n(\eta)}{d\eta} \\ I_n(\eta)\eta^2 C + \frac{1}{L} \frac{dI_n(\eta)}{d\eta} & 0 \end{array} \right) \end{aligned} \quad (69)$$

where  $\mathbf{e}_2$  is a unit vector in the  $y$ -direction and we defined  $C = \frac{e\kappa\beta_b L^2}{2}$ . Calculating the spin dependent part of Eq. (68), we define

$$U_{\uparrow}(y) = \left( \begin{array}{c} I_n(\eta) \\ 0 \\ \frac{p_z I_n(\eta)}{\varepsilon_n + e\varphi(y) + m} \\ \frac{p_x I_n(\eta) + I_n(\eta)\eta^2 C + \frac{1}{L} \frac{dI_n(\eta)}{d\eta}}{\varepsilon_n + e\varphi(y) + m} \end{array} \right), \quad (70)$$

$$U_{\downarrow}(y) = \left( \begin{array}{c} 0 \\ I_n(\eta) \\ \frac{p_x I_n(\eta) + I_n(\eta)\eta^2 C - \frac{1}{L} \frac{dI_n(\eta)}{d\eta}}{\varepsilon_n + e\varphi(y) + m} \\ \frac{-p_z I_n(\eta)}{\varepsilon_n + e\varphi(y) + m} \end{array} \right). \quad (71)$$

Finally, since the potential  $(-e\varphi(y))$  in the denominator is much smaller than the energy  $\varepsilon_n$  (this is the same condition as in subsection IV B) we can make the following approximation, valid when  $\gamma_0 \gg \xi$

$$\begin{aligned} & \frac{p_x I_n(\eta) + I_n(\eta)\eta^2 C + \frac{1}{L} \frac{dI_n(\eta)}{d\eta}}{\varepsilon_n + e\varphi(y) + m} \\ &= \frac{p_x I_n(\eta) + I_n(\eta)\eta^2 C + \frac{1}{L} \frac{dI_n(\eta)}{d\eta}}{(\varepsilon_n + m) \left(1 + \frac{e\varphi(y)}{\varepsilon_n + m}\right)} \\ &\simeq \frac{p_x I_n(\eta) + I_n(\eta)\eta^2 C + \frac{1}{L} \frac{dI_n(\eta)}{d\eta}}{(\varepsilon_n + m)} \left(1 - \frac{e\varphi(y)}{\varepsilon_n + m}\right) \\ &\simeq \frac{p_x I_n(\eta) - \frac{p_x}{\varepsilon_n + m} e\varphi(y) I_n(\eta) + I_n(\eta)\eta^2 C + \frac{1}{L} \frac{dI_n(\eta)}{d\eta}}{\varepsilon_n + m} \\ &\simeq \frac{p_x I_n(\eta) + I_n(\eta)\eta^2 D + \frac{1}{L} \frac{dI_n(\eta)}{d\eta}}{\varepsilon_n + m}, \end{aligned} \quad (72)$$

where  $D = \frac{e\kappa(\frac{p_x}{\varepsilon_n + m} + \beta_b)L^2}{2} \simeq \frac{e\kappa(1 + \beta_b)L^2}{2}$ , and so we obtain

$$U_{\uparrow}(y) = \left( \begin{array}{c} I_n(\eta) \\ 0 \\ \frac{p_z I_n(\eta)}{\varepsilon_n + m} \\ \frac{p_x I_n(\eta) + I_n(\eta)\eta^2 D + \frac{1}{L} \frac{dI_n(\eta)}{d\eta}}{\varepsilon_n + m} \end{array} \right), \quad (73)$$

$$U_{\downarrow}(y) = \left( \begin{array}{c} 0 \\ I_n(\eta) \\ \frac{p_x I_n(\eta) + I_n(\eta)\eta^2 D - \frac{1}{L} \frac{dI_n(\eta)}{d\eta}}{\varepsilon_n + m} \\ \frac{-p_z I_n(\eta)}{\varepsilon_n + m} \end{array} \right), \quad (74)$$

such that our solutions, finally, can be spanned by the two solutions

$$\psi_{\uparrow}(\mathbf{r}, t) = \frac{1}{\sqrt{2L_x L_z}} e^{i(p_x x + p_z z - \varepsilon_n t)} U_{\uparrow}(y) \quad (75)$$

$$\psi_{\downarrow}(\mathbf{r}, t) = \frac{1}{\sqrt{2L_x L_z}} e^{i(p_x x + p_z z - \varepsilon_n t)} U_{\downarrow}(y) \quad (76)$$

It was earlier stated that the normalization was for one particle per area, however unproven. To show that this is correct within our approximation, we calculate  $\int \psi_{\uparrow}^{\dagger}(\mathbf{r}, t) \psi(\mathbf{r}, t) dV$ . We have

$$\begin{aligned} & \int \psi_{\uparrow}^{\dagger}(\mathbf{r}, t) \psi_{\uparrow}(\mathbf{r}, t) dV \\ &= \frac{1}{2} \int dy \left( |I_n(\eta)|^2 + \left[ \frac{p_x I_n(\eta) + I_n(\eta) \eta^2 C + \frac{1}{L} \frac{dI_n(\eta)}{d\eta}}{\varepsilon_n + e\varphi(y) + m} \right]^2 \right) \end{aligned} \quad (77)$$

where the integration over  $dx dz$  has canceled out with the area  $L_x L_z$  in the front factor of Eq. (75). We show here the case up spin-up, but the result is the same for spin-down.

By using the properties that the derivative of the  $I_n(\eta)$  function, as they are harmonic oscillator wave functions, is related to the stepped up and down wave-functions we find that we should add a normalization factor on the wave function of

$$\frac{1}{\sqrt{1 + \frac{p_x^2 - (E_n + m)^2 + (\frac{3}{2}n^2 + \frac{3}{2}n + \frac{3}{4})D^2 + (\frac{1}{L^2} + p_x D)(n + \frac{1}{2})}{2(\varepsilon_n + m)^2}}}. \quad (78)$$

To estimate the size of this correction we also need to know the typical size of  $n$ . The solutions  $I_n(\eta)$  rapidly drop off, for large  $n$ , when beyond the classical turning points which can be found from Eq. (64) and (55) to correspond to  $\eta^2 > 2n + 1$ . We have that  $e(A_x(y) - \varphi(y)) \sim D\eta^2$  and therefore  $nD \sim -e\varphi(y_{\max})$ . Thus we have terms that are on the order of  $-e\varphi(y_{\max})/\varepsilon_n$  or this factor squared, which is therefore of the same size as the correction found in section IV A. The term  $n/L^2$  can be seen to be on the same order by replacing  $n \sim -e\varphi(y_{\max})/D$  and using the definition of  $L$ . Therefore, as long as  $\gamma_0 \gg \xi$  the normalization of Eq. (75) and (76) is correct within our accuracy.

## V. RADIATION EMISSION

Now that we have obtained the wave-functions we can calculate the probability of radiation emission by using the transition matrix element from an initial state  $\psi_i(x)$  to a final state  $\psi_f(x)$  while emitting a photon with momentum four-vector  $k^{\mu} = (\omega, \mathbf{k})$  and polarization  $\epsilon$ , which is given by

$$S_{fi} = \int d^4x \bar{\psi}_f(x) i e \sqrt{\frac{4\pi}{2\omega V}} \not{\epsilon}^* e^{ikx} \psi_i(x). \quad (79)$$

Then the differential rate of emission  $dW$  is usually given by

$$dW = |S_{fi}|^2 \frac{1}{T} \frac{V d^3 p_f}{(2\pi)^3} \frac{V d^3 k}{(2\pi)^3}, \quad (80)$$

where  $V$  is the normalization volume and  $T$  the interaction time, factors which eventually cancel out. In our case the density of final states of the electron instead becomes  $\frac{V d^3 p_f}{(2\pi)^3} \rightarrow \frac{dp_x dp_z L_x L_z}{(2\pi)^2} \sum_{n_f}$ , where  $L_x L_z$  is a normalization area. This change is due simply to the fact that one quantum number is discrete instead of continuous. Inserting our wave-functions from Eq. (76) we obtain

$$\begin{aligned} S_{fi} &= i e \sqrt{\frac{4\pi}{2\omega V}} \frac{1}{2L_x L_z} \int d^4x \bar{U}_f(y) \not{\epsilon}^* U_i(y) \\ &\times e^{-ik_y y} e^{i(p_{x,i} - p_{x,f} - k_x)x} e^{i(p_{z,i} - p_{z,f} - k_z)z} \\ &\times e^{i(\varepsilon_f + \omega - \varepsilon_i)t}, \end{aligned} \quad (81)$$

and carrying out the trivial integrations we obtain,

$$\begin{aligned} S_{fi} &= i e \sqrt{\frac{4\pi}{2\omega V}} \frac{1}{2L_x L_z} (2\pi)^3 \int \bar{U}_f(y) \not{\epsilon}^* U_i(y) e^{-ik_y y} dy \\ &\times \delta(p_{x,i} - p_{x,f} - k_x) \delta(p_{z,i} - p_{z,f} - k_z) \\ &\times \delta(\varepsilon_f + \omega - \varepsilon_i). \end{aligned} \quad (82)$$

Since we need this quantity squared, we must consider the meaning of the delta-function squared. Here we take the usual approach to obtain factors of the normalization volume and time, i.e.  $[\delta(p_{x,i} - p_{x,f} - k_x) \delta(p_{z,i} - p_{z,f} - k_z) \delta(\varepsilon_f + \omega - \varepsilon_i)]^2 = \frac{L_x L_z T}{(2\pi)^3} \delta(p_{x,i} - p_{x,f} - k_x) \delta(p_{z,i} - p_{z,f} - k_z) \delta(\varepsilon_f + \omega - \varepsilon_i)$  and so we obtain

$$\begin{aligned} |S_{fi}|^2 &= \frac{4\pi e^2}{2\omega V} \frac{1}{(2L_x L_z)^2} (2\pi)^6 \\ &\times \left| \int \bar{U}_f(y) \not{\epsilon}^* U_i(y) e^{-ik_y y} dy \right|^2 \\ &\times \frac{L_x L_z T}{(2\pi)^3} \delta(p_{x,i} - p_{x,f} - k_x) \delta(p_{z,i} - p_{z,f} - k_z) \\ &\times \delta(\varepsilon_f + \omega - \varepsilon_i). \end{aligned} \quad (83)$$

Now integrating over final electron momentum we obtain



$$\begin{aligned}
& \int \frac{dp_x dp_z L_x L_z}{(2\pi)^2} \sum_{n_f} |S_{fi}|^2 \\
&= \sum_{n_f} \frac{4\pi e^2}{2\omega V} \frac{1}{(2L_x L_z)^2} (2\pi)^6 \\
&\times \left| \int \bar{U}_f(y) \not{\epsilon}^* U_i(y) e^{-ik_y y} dy \right|^2 \\
&\times \frac{L_x L_z T}{(2\pi)^3} \frac{L_x L_z}{(2\pi)^2} \delta(\varepsilon_f + \omega - \varepsilon_i) \\
&= \sum_{n_f} \frac{e^2}{4\omega V} (2\pi)^2 \left| \int \bar{U}_f(y) \not{\epsilon}^* U_i(y) e^{-ik_y y} dy \right|^2 \\
&\times T \delta(\varepsilon_f + \omega - \varepsilon_i).
\end{aligned} \tag{84}$$

Now we must only add the photon density of states from Eq. (80) and we obtain the differential rate as

$$\begin{aligned}
dW &= \sum_{n_f} \frac{e^2}{8\pi\omega} \left| \int \bar{U}_f(y) \not{\epsilon}^* U_i(y) e^{-ik_y y} dy \right|^2 \\
&\times \delta(\varepsilon_f + \omega - \varepsilon_i) \omega^2 d\omega d\Omega.
\end{aligned} \tag{85}$$

Now we wish to integrate over  $d\cos\theta$  in  $d\Omega = d\Phi d\cos\theta$  to get rid of the last delta-function. To do this we use the energy relation of Eq. (64) to write the final energy and use that the momentum delta functions have fixed  $p_{x,f} = p_{x,i} - k_x$  and  $p_{z,f} = p_{z,i} - k_z$ . Now writing the photon momentum vector  $\mathbf{k}$  in spherical coordinates,

$$\mathbf{k} = \omega(\cos\theta, \sin\theta\cos\Phi, \sin\theta\sin\Phi), \tag{86}$$

we have that

$$p_{z,f} = -k_z = -\omega\sin\theta\sin\Phi, \tag{87}$$

$$p_{x,f} = p_{x,i} - \omega\cos\theta. \tag{88}$$

In this case Eq. (64) for the final energy  $\varepsilon_f$  becomes

$$\begin{aligned}
\varepsilon_f^2 &= (2n+1) \sqrt{e\kappa(p_{x,i} + \varepsilon_i - \omega(1 + \cos\theta))} \\
&+ (p_{x,i} - \omega\cos\theta)^2 + \omega^2 \sin^2\theta \sin^2\Phi + m^2.
\end{aligned} \tag{89}$$

Now we wish to carry out the integration over  $d\cos\theta$  so we must transform the delta function so

$$\delta(\varepsilon_f(\cos\theta) + \omega - \varepsilon_i) = \frac{\delta(\cos\theta - \cos\theta_0)}{\left| \frac{d\varepsilon_f}{d\cos\theta}(\cos\theta) \right|}, \tag{90}$$

where  $\cos\theta_0$  is the solution to the equation

$$\varepsilon_f(\cos\theta) + \omega - \varepsilon_i = 0, \tag{91}$$

which we will find later. We obtain from Eq. (89)

$$\begin{aligned}
2\varepsilon_f \frac{d\varepsilon_f}{d\cos\theta} &= (2n+1) \frac{-e\kappa\omega}{2\sqrt{e\kappa(p_{x,i} + \varepsilon_i - \omega(1 + \cos\theta))}} \\
&+ 2(p_{x,i} - \omega\cos\theta)(-\omega) \\
&+ \omega^2 \sin^2\Phi \frac{d}{d\cos\theta}(\sin^2\theta),
\end{aligned} \tag{92}$$

from which we can isolate  $\frac{d\varepsilon_f}{d\cos\theta}$ .

$$\begin{aligned}
\frac{d\varepsilon_f}{d\cos\theta} &= \frac{1}{\varepsilon_f} \left( -(2n+1) \frac{e\kappa\omega}{4\sqrt{e\kappa(p_{x,i} + \varepsilon_i - \omega(1 + \cos\theta))}} \right. \\
&\left. - \omega p_{x,i} + \omega^2 \cos\theta \cos^2\Phi \right).
\end{aligned} \tag{93}$$

And so we have integrated over all the delta functions and can write the differential rate as

$$dW = \sum_{n_f} \frac{e^2}{8\pi\omega'} \left| \int \bar{U}_f(y) \not{\epsilon}^* U_i(y) e^{-ik_y y} dy \right|^2 \frac{1}{\left| \frac{d\varepsilon_f}{d\cos\theta} \right|} \omega^2 d\omega d\Phi. \tag{94}$$

To find the solution of Eq. (91) we will recall that we consider ultra-relativistic particles such that  $\theta$  is small meaning we can perform the series expansions of  $\cos\theta \simeq 1 - \frac{\theta^2}{2}$  and  $\sin\theta \simeq \theta$ . Inserting this in Eq. (89) we obtain

$$\begin{aligned}
(\varepsilon_i - \omega)^2 &= (2n+1) \sqrt{e\kappa(p_{x,i} + \varepsilon_i - \omega(2 - \frac{\theta^2}{2}))} \\
&+ (p_{x,i} - \omega + \omega\frac{\theta^2}{2})^2 + \omega^2 \theta^2 \sin^2\Phi + m^2,
\end{aligned} \tag{95}$$

which leads us to the sought after solution of Eq. (91)

$$\begin{aligned}
\theta_0 &= \left[ (\varepsilon_i - \omega)^2 - (2n+1) \sqrt{e\kappa(p_{x,i} + \varepsilon_i - 2\omega)} \right. \\
&\left. - (p_{x,i} - \omega)^2 - m^2 \right]^{1/2} \\
&/ \left[ (p_{x,i} - \omega)\omega + \omega^2 \sin^2\Phi \right. \\
&\left. + \frac{\omega/4}{p_{x,i} + \varepsilon_i - 2\omega} (2n+1) \sqrt{e\kappa(p_{x,i} + \varepsilon_i - 2\omega)} \right]^{1/2}.
\end{aligned} \tag{96}$$

Now we have all the quantities necessary to evaluate the rate from Eq. (94).

## VI. BAIER METHOD

From [46] it can be seen that the differential power emitted in the semi-classical operator method is given by

$$\begin{aligned} \frac{d^2 P}{d\omega d\Omega} &= \frac{1}{T} \frac{e^2}{4\pi^2} \omega'^2 \left( \frac{\varepsilon^2 + \varepsilon'^2}{2\varepsilon^2} \left| \int_{-\infty}^{\infty} (\mathbf{n} - \mathbf{v}) e^{i\omega'(t-\mathbf{n}\cdot\mathbf{r})} dt \right|^2 \right. \\ &\quad \left. + \frac{\omega^2 m^2}{2\varepsilon^4} \left| \int_{-\infty}^{\infty} e^{i\omega'(t-\mathbf{n}\cdot\mathbf{r})} dt \right|^2 \right), \end{aligned} \quad (97)$$

where  $\varepsilon' = \varepsilon - \omega$ ,  $\omega' = \omega\varepsilon/(\varepsilon - \omega)$ ,  $\mathbf{n} = (\cos\theta, \sin\theta\cos\Phi, \sin\theta\sin\Phi)$  is the direction of emission and  $\mathbf{r}(t)$  and  $\mathbf{v}(t)$  are the classical position and velocity vectors, respectively. It is beneficial to first look at the integral from the second term and insert the motion found in section III

$$\begin{aligned} &\int_{-\infty}^{\infty} e^{i\omega'(t-\mathbf{n}\cdot\mathbf{r})} dt \\ &= \int_{-\infty}^{\infty} e^{i\omega'(t-\cos\theta) \left[ \left(1 - \frac{1}{2\gamma_0^2} - \frac{\xi^2}{4\gamma_0^2}\right)t - \frac{1}{4} \left(\frac{\xi}{\gamma_0}\right)^2 \frac{\sin(2\omega_0 t)}{2\omega_0} \right]} \\ &\quad \times e^{-i\omega' \sin\theta \cos\Phi \frac{\xi}{\gamma_0 \omega_0} \sin(\omega_0 t)} dt. \end{aligned} \quad (98)$$

If we change variable to  $\tau = \omega_0 t$  and expand  $\cos\theta$  as earlier this can be rewritten as

$$\begin{aligned} &\int_{-\infty}^{\infty} e^{i\omega'(t-\mathbf{n}\cdot\mathbf{r})} dt \\ &= \frac{1}{\omega_0} \int e^{i\omega' \left( \frac{\tau}{2\gamma_0^2 \omega_0} [1 + \frac{1}{2}\xi^2 + \gamma_0^2 \theta^2] \right)} \\ &\quad \times e^{i\omega' \left( \frac{1}{8\omega_0} \left(\frac{\xi}{\gamma_0}\right)^2 \sin(2\tau) - \sin\theta \cos\Phi \frac{\xi}{\gamma_0 \omega_0} \sin(\tau) \right)} d\tau. \end{aligned} \quad (99)$$

Now we know that

$$e^{i\omega' \left( \frac{1}{8\omega_0} \left(\frac{\xi}{\gamma_0}\right)^2 \sin(2\tau) - \sin\theta \cos\Phi \frac{\xi}{\gamma_0 \omega_0} \sin(\tau) \right)}, \quad (100)$$

is a  $2\pi$  periodic function so we can write it as a Fourier series

$$e^{i\omega' \left( \frac{1}{8\omega_0} \left(\frac{\xi}{\gamma_0}\right)^2 \sin(2\tau) - \sin\theta \cos\Phi \frac{\xi}{\gamma_0 \omega_0} \sin(\tau) \right)} = \sum_{n=-\infty}^{\infty} c_n e^{-in\tau}, \quad (101)$$

with coefficients given by

$$\begin{aligned} c_n &= \frac{1}{2\pi} \int_{-\pi}^{\pi} e^{i \left( n\tau + \frac{\omega'}{8\omega_0} \left(\frac{\xi}{\gamma_0}\right)^2 \sin(2\tau) - \sin\theta \cos\Phi \frac{\omega' \xi}{\gamma_0 \omega_0} \sin(\tau) \right)} \\ &= A_0(-n, -\alpha_1, -\alpha_2) = A_0(n, \alpha_1, \alpha_2), \end{aligned} \quad (102)$$

where we have defined

$$\begin{aligned} A_m(n, \alpha_1, \alpha_2) &= \frac{1}{2\pi} \int_{-\pi}^{\pi} \cos^m(\tau) e^{i(\alpha_1 \sin(\tau) - \alpha_2 \sin(2\tau) - n\tau)} d\tau, \end{aligned} \quad (103)$$

as in [2, 26], with

$$\alpha_1 = \sin\theta \cos\Phi \frac{\omega' \xi}{\gamma_0 \omega_0}, \quad (104)$$

and

$$\alpha_2 = \frac{\omega'}{8\omega_0} \left( \frac{\xi}{\gamma_0} \right)^2. \quad (105)$$

When inserting this in Eq. (99) we obtain

$$\begin{aligned} &\int_{-\infty}^{\infty} e^{i\omega'(t-\mathbf{n}\cdot\mathbf{r})} dt \\ &= \frac{1}{\omega_0} \sum_{n=-\infty}^{\infty} c_n \int e^{i\tau \left( \frac{\omega'}{2\gamma_0^2 \omega_0} [1 + \frac{1}{2}\xi^2 + \gamma_0^2 \theta^2] - n \right)} d\tau \\ &= \frac{2\pi}{\omega_0} \sum_{n=-\infty}^{\infty} A_0(n, \alpha_1, \alpha_2) \delta \left( \frac{\omega'}{2\gamma_0^2 \omega_0} \left( 1 + \frac{1}{2}\xi^2 + \gamma_0^2 \theta^2 \right) - n \right). \end{aligned} \quad (106)$$

Now calculating  $\int_{-\infty}^{\infty} (\mathbf{n} - \mathbf{v}) e^{i\omega'(t-\mathbf{n}\cdot\mathbf{r})} dt$  is straightforward. For the  $y$ -component we have

$$\begin{aligned} &\int_{-\infty}^{\infty} (\mathbf{n} - \mathbf{v})_y e^{i\omega'(t-\mathbf{n}\cdot\mathbf{r})} dt \\ &= \int_{-\infty}^{\infty} \left( \sin\theta \cos\Phi - \frac{\xi}{\gamma_0} \cos(\omega_0 t) \right) \\ &\quad \times e^{i\omega'(t - \cos\theta v_0 t - \sin\theta \cos\Phi \frac{\xi}{\gamma_0 \omega_0} \sin(\omega_0 t))} dt. \end{aligned} \quad (107)$$

The first term is simply a constant (no  $\tau$  dependence) times the integral we have already calculated, and the cosine factor in the second term means we simply need to replace  $A_0(n, \alpha_1, \alpha_2)$  with  $A_1(n, \alpha_1, \alpha_2)$  and so

$$\begin{aligned} &\int_{-\infty}^{\infty} (\mathbf{n} - \mathbf{v})_y e^{i\omega'(t-\mathbf{n}\cdot\mathbf{r})} dt \\ &= \frac{2\pi}{\omega_0} \sum_{n=-\infty}^{\infty} \left[ \sin\theta \cos\Phi A_0(n, \alpha_1, \alpha_2) - \frac{\xi}{\gamma_0} A_1(n, \alpha_1, \alpha_2) \right] \\ &\quad \times \delta \left( \frac{\omega'}{2\gamma_0^2 \omega_0} \left( 1 + \frac{1}{2}\xi^2 + \gamma_0^2 \theta^2 \right) - n \right). \end{aligned} \quad (108)$$

The  $z$ -component is simply a constant times the result from Eq. (106), since  $v_z = 0$ , so we have

$$\begin{aligned} & \int_{-\infty}^{\infty} (\mathbf{n} - \mathbf{v})_z e^{i\omega'(t-\mathbf{n}\cdot\mathbf{r})} dt \\ &= \frac{2\pi}{\omega_0} \sum_{n=-\infty}^{\infty} \sin\theta \sin\Phi A_0(n, \alpha_1, \alpha_2) \\ & \times \delta\left(\frac{\omega'}{2\gamma_0^2\omega_0} \left(1 + \frac{1}{2}\xi^2 + \gamma_0^2\theta^2\right) - n\right). \end{aligned} \quad (109)$$

In Eq. (97) we see that we need these quantities squared and so we must consider the meaning of the delta function  $\delta\left(\frac{\omega'}{2\gamma_0^2\omega_0} \left(1 + \frac{1}{2}\xi^2 + \gamma_0^2\theta^2\right) - n\right)$  squared. This came from an integral over the phase  $\tau$  and so the usual approach is that

$$\begin{aligned} & \left[ \delta\left(\frac{\omega'}{2\gamma_0^2\omega_0} \left(1 + \frac{1}{2}\xi^2 + \gamma_0^2\theta^2\right) - n\right) \right]^2 \\ &= \delta\left(\frac{\omega'}{2\gamma_0^2\omega_0} \left(1 + \frac{1}{2}\xi^2 + \gamma_0^2\theta^2\right) - n\right) \frac{\Delta\tau}{2\pi}, \end{aligned} \quad (110)$$

where  $\Delta\tau$  is the phase-length which is  $\omega_0 T$  where  $T$  is the interaction time, which we can divide with on both sides of Eq. (97) to obtain the energy emitted per unit time. We therefore obtain that

$$\begin{aligned} & \left| \int (\mathbf{n} - \mathbf{v}) e^{i\omega'(t-\mathbf{n}\cdot\mathbf{r})} dt \right|^2 \\ &= \frac{(2\pi)^2 T\omega_0}{\omega_0^2} \frac{1}{2\pi} \delta\left(\frac{\omega'}{2\gamma_0^2\omega_0} \left(1 + \frac{1}{2}\xi^2 + \gamma_0^2\theta^2\right) - n\right) \\ & \times \sum_{n=-\infty}^{\infty} \left[ \sin\theta \cos\Phi A_0(n, \alpha_1, \alpha_2) - \frac{\xi}{\gamma_0} A_1(n, \alpha_1, \alpha_2) \right]^2 \\ & + [\sin\theta \sin\Phi A_0(n, \alpha_1, \alpha_2)]^2. \end{aligned} \quad (111)$$

Now we wish to carry out the integration over  $d\theta$  so we recognize that the content of the delta function is a function of  $\theta$  which we define as  $g(\theta)$  to use the formula  $\delta(g(\theta)) = \delta(\theta - \theta_{0,B}) / \left| \frac{dg}{d\theta}(\theta_{0,B}) \right|$  where  $\theta_{0,B}$  is the solution to  $g(\theta_{0,B}) = 0$ . So

$$g(\theta) = \frac{\omega'}{2\gamma_0^2\omega_0} \left(1 + \frac{1}{2}\xi^2 + \gamma_0^2\theta^2\right) - n, \quad (112)$$

$$g'(\theta) = \frac{\omega'}{\omega_0} \theta, \quad (113)$$

and we then find the zero as

$$\theta_{0,B} = \frac{1}{\gamma_0} \sqrt{\frac{2\gamma_0^2\omega_0 n}{\omega'} - \left(1 + \frac{\xi^2}{2}\right)}. \quad (114)$$

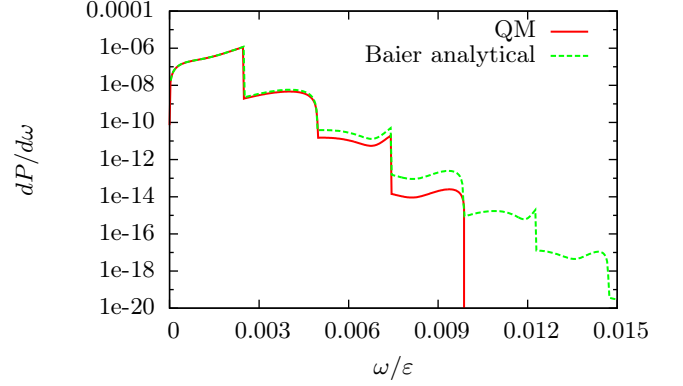


Figure 2: The case of  $n = 4$  and  $\xi = 0.1$ . The label 'QM' refers to the fully quantum calculation and 'Baier analytical' to the semi-classical method of Baier & Katkov.

The other solution,  $-\theta_{0,B}$  is not allowed by our choice of coordinate system where  $0 \leq \theta \leq \pi$ . Here we see that we should have  $n \geq 1$  to have any solutions. Once again approximating  $\sin\theta \simeq \theta$  we have that

$$\begin{aligned} & \int d\Phi d\theta \left| \int (\mathbf{n} - \mathbf{v}) e^{i\omega'(t-\mathbf{n}\cdot\mathbf{r})} dt \right|^2 \\ &= \int d\Phi \frac{2\pi T}{\omega'} \sum_{n=-\infty}^{\infty} \left[ \theta_{0,B} \cos\Phi A_0(n, \alpha_1, \alpha_2) - \frac{\xi}{\gamma_0} A_1(n, \alpha_1, \alpha_2) \right]^2 \\ & + [\theta_{0,B} \sin\Phi A_0(n, \alpha_1, \alpha_2)]^2, \end{aligned} \quad (115)$$

and for the second term of Eq. (97), we obtain

$$\begin{aligned} & \left| \int e^{i\omega'(t-\mathbf{n}\cdot\mathbf{r})} dt \right|^2 = \frac{2\pi}{\omega_0^2} T\omega_0 \sum_{n=-\infty}^{\infty} A_0^2(n, \alpha_1, \alpha_2) \\ & \times \delta\left(\frac{\omega'}{2\gamma_0^2\omega_0} \left(1 + \frac{1}{2}\xi^2 + \gamma_0^2\theta^2\right) - n\right). \end{aligned} \quad (116)$$

Integrating this term over all angles as well, we obtain

$$\begin{aligned} & \int d\Phi d\theta \left| \int e^{i\omega'(t-\mathbf{n}\cdot\mathbf{r})} dt \right|^2 \\ &= \int d\Phi \frac{2\pi T}{\omega'} \sum_{n=-\infty}^{\infty} A_0^2(n, \alpha_1, \alpha_2). \end{aligned} \quad (117)$$

So in total we obtain the emitted power  $dP$  (energy per unit time) differential in the emitted photon energy as

$$\begin{aligned}
\frac{dP}{d\omega} &= \frac{e^2}{2\pi} \omega' \int d\Phi \sum_{n=1}^{\infty} \\
&\times \left( \frac{\varepsilon'^2 + \varepsilon^2}{2\varepsilon^2} \left[ \left\{ \theta_{0,B} \cos\Phi A_0(n, \alpha_1, \alpha_2) - \frac{\xi}{\gamma_0} A_1(n, \alpha_1, \alpha_2) \right\}^2 \right. \right. \\
&+ \left. \left. \left\{ \theta_{0,B} \sin\Phi A_0(n, \alpha_1, \alpha_2) \right\}^2 \right] \right. \\
&+ \left. \frac{\omega^2 m^2}{2\varepsilon^4} A_0^2(n, \alpha_1, \alpha_2) \right). \tag{118}
\end{aligned}$$

In this form it is clear which terms correspond to which from Eq. (97), however it is not immediately obvious that it is identical to that found in [26]. To obtain this we must carry out the square in the term  $\left\{ \theta_{0,B} \cos\Phi A_0(n, \alpha_1, \alpha_2) - \frac{\xi}{\gamma_0} A_1(n, \alpha_1, \alpha_2) \right\}^2$ . This will give us a term  $-2\theta_{0,B} \cos\Phi A_0(n, \alpha_1, \alpha_2) \frac{\xi}{\gamma_0} A_1(n, \alpha_1, \alpha_2)$  which we will rewrite by employing the relation found in [2] stating that

$$\begin{aligned}
\alpha_1 A_1(n, \alpha_1, \alpha_2) &= (n - 2\alpha_2) A_0(n, \alpha_1, \alpha_2) \\
&+ 4\alpha_2 A_2(n, \alpha_1, \alpha_2), \tag{119}
\end{aligned}$$

and from this we can express  $\cos\Phi A_1(n, \alpha_1, \alpha_2)$  in terms of  $A_0$  and  $A_2$ , which after some rewriting will lead us to the expected result

$$\begin{aligned}
\frac{dP}{d\omega} &= \frac{e^2}{2\pi} \frac{\omega}{\gamma_0^2} \int d\Phi \sum_{n=1}^{\infty} \\
&\times \left( -A_0^2 + \xi^2 \left( 1 + \frac{u^2}{2(1+u)} \right) (A_1^2 - A_0 A_2) \right), \tag{120}
\end{aligned}$$

where  $u = \frac{\omega}{\varepsilon - \omega}$ .

## VII. RESULTS AND DISCUSSION

Now we have calculated the radiation emission using two different approaches to the same problem. One is fully quantum mechanical, and the other a semi-classical approach. A third method which is well known in the literature [62–65] is to approximate the emission as happening in a constant crossed field and use the formula for radiation emission in this case. This is generally considered applicable when  $\xi \gg 1$  and so we will also make this comparison when this condition is fulfilled.

When dealing with radiation emission the quantum parameter is defined by

$$\chi = \frac{e\sqrt{-(F^{\mu\nu}p_\nu)^2}}{m^3}, \tag{121}$$

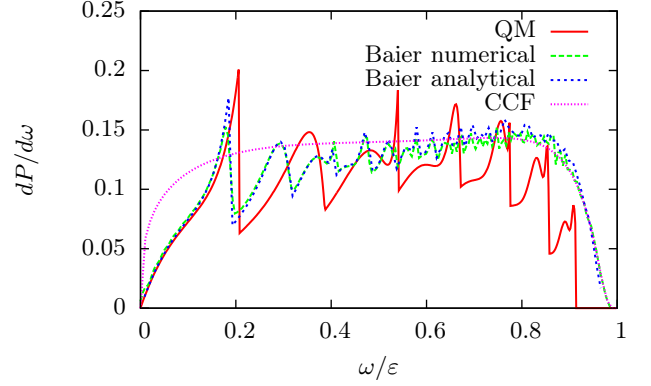


Figure 3: The case of  $n = 8$ ,  $\xi = 5$ ,  $\chi = 7.81$ . The label 'QM' refers to the fully quantum calculation, 'Baier numerical' to the semi-classical method of Baier & Katkov for 15 periods of oscillation, 'Baier analytical' to the analytical results obtained from the semi-classical method corresponding to the limit of many oscillations, and the label 'CCF' corresponds to the constant crossed field approximation. This figure shows the 'doubly quantum' regime where the semi-classical method breaks down.

and tells us how important quantum effects such as recoil and spin are. When  $\chi \ll 1$  these effects are small. However the effect of low quantum number is not covered by this parameter, and is a separate condition. We will consider the peak value in terms of the parameters of our problem which is then given by

$$\chi_{\max} = \kappa y_{\max} \frac{2\gamma_0}{E_c}, \tag{122}$$

where  $E_c = \frac{m^2}{e}$  is the Schwinger critical field. From the wave-functions seen in Eq. (75) we know that the harmonic oscillator function  $I_n(\eta)$  will start tending towards 0 when  $\eta > \sqrt{2n}$ , corresponding to the classical amplitude of oscillation. Thus  $y_{\max}$  can also be accurately written as  $y_{\max} = L\sqrt{2n}$  when  $n$  is large so

$$\chi_{\max} = \kappa\sqrt{2n}L \frac{2\gamma_0}{E_c}. \tag{123}$$

Setting  $p_x \simeq \varepsilon$  and  $\beta_b \simeq 1$  we have

$$\frac{1}{L} \simeq \sqrt[4]{2\epsilon\kappa p_x}, \tag{124}$$

$$\frac{1}{2p_x L^4} = \epsilon\kappa \tag{125}$$

and so we have that

$$\chi_{\max} = \sqrt{2n} \left( \frac{\lambda_C}{L} \right)^3, \tag{126}$$

where  $\lambda_C = 1/m$  is the Compton wavelength. In the special case of the harmonic oscillator, the momentum

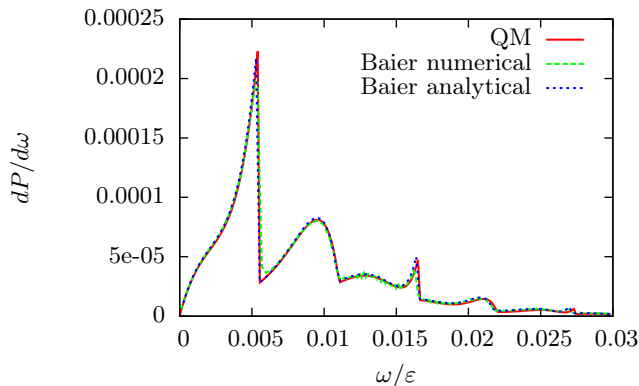


Figure 4: The case of  $n = 120$ ,  $\xi = 1$ . The label 'QM' refers to the fully quantum calculation, 'Baier numerical' to the semi-classical method of Baier & Katkov for 15 periods of oscillation, 'Baier analytical' to the analytical results obtained from the semi-classical method corresponding to the limit of many oscillations. Here we see how for quite large values of the quantum number the semi-classical method is good.

space wave-function is the same as the space wave function save only for a different variable, such that instead of  $I_n(y/L)$  we have  $I_n(q_y L)$  and therefore since the function  $I_n(\eta)$  decreases rapidly for  $\eta^2 > 2n$  we can also write  $q_{y,\max}^2 = 2n/L^2$ . And so we express the other parameter usually considered when dealing with radiation emission  $\xi$  in terms of the parameters of our solutions to obtain that

$$\xi = \frac{q_{y,\max}}{m} = \frac{\lambda_C}{L} \sqrt{2n}. \quad (127)$$

And combining this with Eq. (126) we obtain the useful relation

$$\chi_{\max} = \frac{\xi^3}{2n}. \quad (128)$$

For weak fields, meaning a small field gradient  $\kappa$ ,  $L$  will become large, and so we will denote  $L \gg \lambda_C$  as the weak field gradient regime and vice versa. Below we will discuss features of the radiation spectrum shown in the figures in the different regimes. In the figures the label 'QM' corresponds to the exact calculation of Eq. (94), 'Baier analytical' corresponds to Eq. (120). 'Baier numerical' corresponds to using the formula of Eq. (97) by numerically solving the equations of motion corresponding to a time of 15 oscillations in the field numerically, and then performing the integration over angles and time numerically as done in [46]. The label 'CCF' corresponds to the radiation emitted when applying the constant crossed field approximation.

### A. Weak field gradient regime, $L \gg \lambda_C$

In this regime when the quantum number  $n$  is small, both  $\chi_{\max}$  and  $\xi$  will be small as seen from Eq. (126) and Eq. (127). A small value of  $\chi_{\max}$  means the only quantum effects for  $n$  small are those due to the quantization of the motion. Since  $\xi$  will be small, the radiation is in the dipole regime, meaning different harmonics are clear and most radiation comes from the first harmonic. In figure 2 we have shown a plot of the radiation spectrum in this regime using the exact calculation and the semi-classical approximation. Coincidentally the two calculations yield same result for the first harmonic, and differences are only seen for higher harmonics. So differences are only seen in the parts of the spectrum where the radiation yield is small. Another difference is that the exact calculation only allows a finite number of harmonics corresponding to transitions from the initial state with quantum number  $n_i$  to one with lower quantum number, and the last harmonic thus corresponds to transition to the ground state and for photon energies above the threshold corresponding to this harmonic, no radiation can be emitted. With the semi-classical method this is not the case and the sum over harmonics is infinite. This case of the weak field gradient regime is the regime of planar channeling of positrons for low energies. For channeling of relativistic positrons, the positron also experiences a potential which is close to parabolic. However in channeling, low quantum numbers for the motion can only be achieved while one is also in the dipole regime. Therefore in [26] there is a section on calculating the (dominant) radiation from the first harmonic in this regime of low quantum numbers which does not use their developed semi-classical method. Although planar channeling of positrons is in this regime, we think that it would be difficult to see the effects seen in figure 2 because the slight anharmonicity of the true potential would also yield contributions at higher harmonics, which would likely be larger than these effects.

### B. Strong field gradient regime, $L \ll \lambda_C$

If one wants to see big differences in the whole of the spectrum as seen in figure 3, one must be in the strong field regime and have small value of  $n$ . In this regime one will always have large  $\chi$  such that recoil and spin is important, and for small  $n$  one has the additional quantum effect of the quantized motion i.e. one needs the wave-function instead of the trajectory.

In figure 3 we have shown an example of this which could be dubbed the "doubly quantum regime", where it is seen that the correct calculation deviates significantly from the constant crossed field approximation (CCF) but also from the result of the semi-classical operator method which is more general, but evidently fails in the regime of low quantum numbers. This transition from the usual regime to the doubly quantum regime happens when the

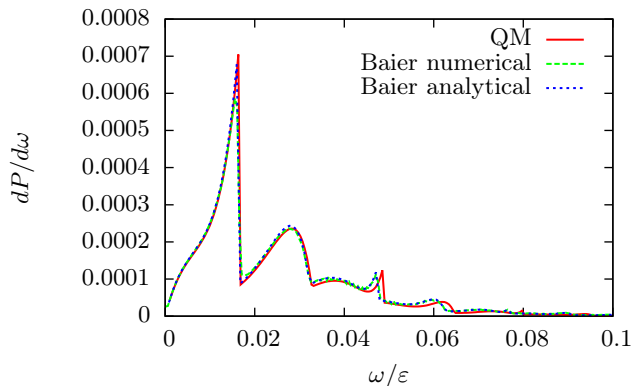


Figure 5: The case of  $n = 40$ ,  $\xi = 1$ . The label 'QM' refers to the fully quantum calculation, 'Baier numerical' to the semi-classical method of Baier & Katkov for 15 periods of oscillation, 'Baier analytical' to the analytical results obtained from the semi-classical method corresponding to the limit of many oscillations. Here we see how for smaller values of the quantum number one begins to see small deviations between the semi-classical method and the correct result.

$n$  quantum number is small and  $L = \frac{1}{m}$  which can be related to a certain beam density as we will see below.

In figure 4 and figure 5 we show the radiation spectrum for  $\xi = 1$  but for a different value of the quantum number  $n$  of the radiating particles. Here it is seen that as  $n$  is large as in the  $n = 120$  case the agreement between the exact calculation and the semi-classical approach is good while when it becomes smaller, in the case of  $n = 40$  the agreement becomes worse. In figure 6 we show the radiation spectrum in the regime where the constant crossed field approximation is applicable and see that while there are small differences between the semi-classical method and the exact calculation in the position of the harmonics, see e.g. the position of 3rd and 4th harmonic peak, the overall size of the spectrum coincides quite well, while the CCF approximation seems to slightly overestimate the radiation emitted at low frequencies. So to see major differences one needs an even smaller value of  $n$  as is the case seen in figure 3.

### C. Beam parameter considerations

To gain an understanding of when these new effects could arise in beamstrahlung, we wish to approximate the parameters we have introduced in terms of the usually given beam parameters, see table I. From Eq. (8) we have that  $\kappa$  relates to the peak density as

$$\kappa = 4\pi\rho_0, \quad (129)$$

where  $\rho_0 = \rho(0, 0, 0)$ . So using Eq. (125) we have that

$$\frac{1}{L^4} = 8\pi e\rho_0\varepsilon. \quad (130)$$

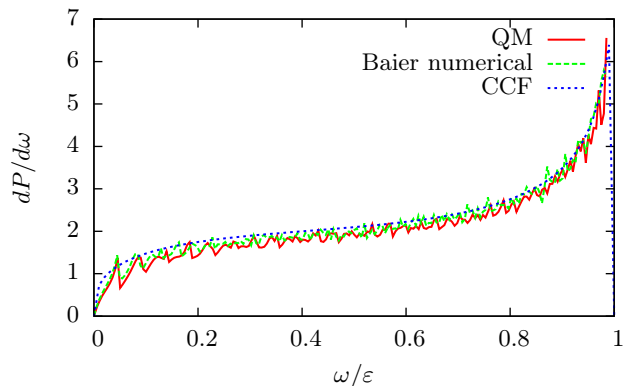


Figure 6: The case of  $n = 40$ ,  $\xi = 30$ . The label 'QM' refers to the fully quantum calculation, 'Baier numerical' to the semi-classical method of Baier & Katkov for 15 periods of oscillation and 'CCF' to the constant crossed field approximation. Here we see how, also in the regime where the CCF approximation may be applied, the deviation from the correct results is small when  $n = 40$ .

Now we can define the critical density  $\rho_c$  as that corresponding to  $L = 1/m$  so  $m^4 = 8\pi e\rho_c\varepsilon$ , or

$$\rho_c = \frac{m^4}{8\pi e\varepsilon}. \quad (131)$$

So to be in the doubly quantum regime one should reach this density and have a small quantum number, i.e. that the transverse beam size becomes comparable to the Compton wavelength. This also gives us another way of expressing the length parameter of the problem  $L$  in terms of the critical density since

$$\frac{1}{L^4} = m^4 \frac{\rho_0}{\rho_c}, \quad (132)$$

and so we also have that

$$\left(\frac{\lambda_C}{L}\right)^4 = \frac{\rho_0}{\rho_c}. \quad (133)$$

Now we can use Eq. (126) to obtain an estimate of the quantum number corresponding to the particles with the largest amplitude, which will contribute most to the radiation spectrum. This gives us

$$\sqrt{2n_{\max}} = \chi_{\max} / \left(\frac{\rho_0}{\rho_c}\right)^{3/4}. \quad (134)$$

Now we wish to obtain an expression giving us the quantum number corresponding to the largest amplitude of oscillation when crossing a bunch in terms of the usual beam parameters such that we can see how this scales and in what regime these effects would become important. We have that

Machine	CLIC	CLIC	ILC	ILC	HER 2017	CLIC mod.
$\varepsilon$	190 GeV	1500 GeV	100 GeV	250 GeV	4 GeV	1500 GeV
N	$5.2 \times 10^9$	$3.7 \times 10^9$	$2.0 \times 10^{10}$	$2.0 \times 10^{10}$	$6.5 \times 10^{10}$	$3.7 \times 10^9$
$\Sigma_x$	149nm	40nm	904nm	474nm	$10.7 \mu\text{m}$	$4 \mu\text{m}$
$\Sigma_y$	2.9nm	1nm	7.8nm	5.9nm	62nm	10pm
$\Sigma_z$	$70 \mu\text{m}$	$44 \mu\text{m}$	$300 \mu\text{m}$	$300 \mu\text{m}$	5mm	$44 \mu\text{m}$
$\chi_{\text{max}}$	0.32	10.7	0.025	0.12	$1.65 \times 10^{-5}$	0.11
$\rho_{\text{max}}$	$7.13 \times 10^6 \text{eV}^3$	$8.72 \times 10^7 \text{eV}^3$	$3.92 \times 10^5 \text{eV}^3$	$9.89 \times 10^5 \text{eV}^3$	$8.16 \times 10^2 \text{eV}^3$	$8.72 \times 10^7 \text{eV}^3$
$\rho_c$	$1.67 \times 10^{11} \text{eV}^3$	$2.12 \times 10^{10} \text{eV}^3$	$3.18 \times 10^{11} \text{eV}^3$	$1.27 \times 10^{11} \text{eV}^3$	$7.9 \times 10^{12} \text{eV}^3$	$2.12 \times 10^{10} \text{eV}^3$
$\lambda_C/L$	0.081	0.25	0.033	0.0528	0.0032	0.25
$\sqrt{2n_{\text{max}}}$	608	657	674	808	512	6.6
$\xi_{\text{max}}$	49	166	22.5	43	1.63	1.67

Table I: Beam parameters.

$$\begin{aligned} \frac{\rho_0}{\rho_c} &= \frac{Ne}{(2\pi)^{3/2}\Sigma_x\Sigma_y\Sigma_z} \frac{8\pi e\varepsilon}{m^4} \\ &= \frac{8\pi Ne^2\gamma_0}{(2\pi)^{3/2}\Sigma_x\Sigma_y\Sigma_z m^3}. \end{aligned} \quad (135)$$

Now we use Eq. (122) and insert  $\kappa$  from Eq. (8) and set  $y_{\text{max}} = \Sigma_y$

$$\chi_{\text{max}} = \frac{4\gamma_0 Ne^2}{\sqrt{2\pi} m^2 \Sigma_x \Sigma_z},$$

So introducing  $o_i = \Sigma_i m$  we have

$$\begin{aligned} \chi_{\text{max}} / \left( \frac{\rho_0}{\rho_c} \right)^{3/4} &= \frac{4\gamma_0 Ne^2}{\sqrt{2\pi} o_x o_z} \left( \frac{(2\pi)^{3/2} o_x o_y o_z}{8\pi Ne^2 \gamma_0} \right)^{3/4} \\ &= \sqrt[4]{\frac{4}{\sqrt{2\pi}} \frac{(o_x o_y o_z)^{3/4}}{o_x o_z}} (N\gamma_0 e^2)^{1/4}, \end{aligned} \quad (136)$$

and so

$$n_{\text{max}} = \frac{1}{\sqrt[4]{2\pi}} \frac{(o_x o_y o_z)^{3/2}}{(o_x o_z)^2} (N\gamma_0 e^2)^{1/2}. \quad (137)$$

To obtain an expression for  $\xi$  we can use the expression for the amplitude Eq. (27) and set it equal  $\Sigma_y$  so that

$$\xi_{\text{max}} = \Sigma_y \gamma_0 \sqrt{\frac{2e\kappa}{\varepsilon}} = \frac{2}{(2\pi)^{1/4}} \sqrt{\frac{Ne^2 \gamma_0 o_y}{o_x o_z}}. \quad (138)$$

From the fact that  $y_{\text{max}} = L\sqrt{2n}$  and that the transition to the doubly quantum regime happens when  $L \simeq 1/m$  and  $n$  small, we can get an estimate of how small the beam-size has to be. So we have that

$\Sigma_{y,\text{crit}} \simeq 10\lambda_C\sqrt{20} = 17$  pm. Currently the accelerator SuperKEKB has beams with a size of 62 nm while future machines such as CLIC has proposed 1 nm beams. In table I we have shown the beam parameters of a current electron-positron accelerator, superKEKB, along with some that are still on the drawing board namely the CLIC and ILC. From the large value of  $\sqrt{2n_{\text{max}}}$  it is clear that the effects we have seen in this paper will not be important, i.e. the semi-classical method will provide the correct result. If the beams are reshaped, making them even smaller in the  $y$ -direction and larger in the  $x$ -direction,  $n_{\text{max}}$  will go down, as can be seen from Eq. (137). For HER (superKEKB) if we reduce  $\Sigma_y$  by a factor of 100 and increase  $\Sigma_x$  with the same amount, the luminosity is unchanged but we then have  $n_{\text{max}} = 13$ . However, because of the low energy and so, not being close to the critical density  $\rho_c$  we would only be in the weak field gradient regime where  $\chi_{\text{max}} \ll 1$ . To be in the doubly quantum regime we have considered CLIC with 3 TeV center of mass energy and reshaped the beams in the same way. This is the ‘‘CLIC mod.’’ case from table I. Here it is seen that  $\chi_{\text{max}} = 0.11$ , so the usual quantum effects would start to come into play, and at the same time we have a small quantum number of  $n_{\text{max}} = 22$ . This reshaping of the beams would be beneficial since  $\chi$  is reduced while keeping the luminosity the same, thus reducing the emitted energy to beamstrahlung. This is the original purpose of having the bunches shaped like sheets. We see here, that if this strategy is taken to the extreme, one will enter this new regime of radiation emission.

## VIII. CONCLUSION

From first principles we have calculated the radiation emission from a relativistic spin- $\frac{1}{2}$  particle in a harmonic oscillator like potential which showed interesting features, allowing us to find a new regime of radiation emission where another quantum effect besides the usual

ones, come into play, namely the quantization of the motion. This effect is absent in the well studied examples of non-linear Compton scattering in a plane wave where the semi-classical method of Baier and Katkov yields the correct result. Contrary, in the field configuration studied here, the semi-classical operator method fails for low quantum numbers. This is interesting in itself, but we also tried to see when one would enter this regime in the case of beamstrahlung. We found that current machines and the ones currently on the drawing board are far away from being in this regime, however if the strategy of making bunches shaped like sheets, which is the

strategy to avoid energy loss due to beamstrahlung, is taken to the extreme, one enters this new regime of radiation emission where the quantization of the motion of the radiating particle becomes important.

## IX. ACKNOWLEDGMENTS

This work was partially supported by a research grant (VKR023371) from VILLUM FONDEN.

- 
- [1] H Mitter. *Acta Phys. Austriaca*, Suppl. XIV:397, 1975.
- [2] V. I. Ritus. *J. Sov. Laser Res.*, 6:497, 1985.
- [3] F Ehlötzky, K Krajewska, and J Z Kamiński. *Rep. Progr. Phys.*, 72:046401, 2009.
- [4] A. Di Piazza, C. Müller, K. Z. Hatsagortsyan, and C. H. Keitel. *Rev. Mod. Phys.*, 84:1177, 2012.
- [5] S. P. Roshchupkin, A. A. Lebed', E. A. Padusenko, and A. I. Voroshilo. *Laser Phys.*, 22:1113, 2012.
- [6] James J. Klein and B. P. Nigam. Birefringence of the vacuum. *Phys. Rev.*, 135:B1279–B1280, Sep 1964.
- [7] Victor Dinu, Tom Heinzl, Anton Ilderton, Mattias Marklund, and Greger Torgrimsson. Vacuum refractive indices and helicity flip in strong-field QED. *Phys. Rev. D*, 89:125003, Jun 2014.
- [8] Thomas Heinzl, Ben Liesfeld, Kay-Uwe Amthor, Heinrich Schwörer, Roland Sauerbrey, and Andreas Wipf. On the observation of vacuum birefringence. *Optics Communications*, 267(2):318 – 321, 2006.
- [9] Stephen L Adler. Vacuum birefringence in a rotating magnetic field. *Journal of Physics A: Mathematical and Theoretical*, 40(5):F143, 2007.
- [10] Tobias N. Wistisen and Ulrik I. Uggerhøj. Vacuum birefringence by Compton backscattering through a strong field. *Phys. Rev. D*, 88:053009, Sep 2013.
- [11] Sergey Bragin, Sebastian Meuren, Christoph H. Keitel, and Antonino Di Piazza. High-energy vacuum birefringence and dichroism in an ultrastrong laser field. *Phys. Rev. Lett.*, 119:250403, Dec 2017.
- [12] N. B. Narozhny and M. S. Fofanov. *J. Exp. Theor. Phys.*, 90:415, 2000.
- [13] S. P. Roshchupkin. *Phys. At. Nucl.*, 64:243, 2001.
- [14] Thomas Heinzl, Anton Ilderton, and Mattias Marklund. *Phys. Lett. B*, 692:250, 2010.
- [15] Tim-Oliver Müller and Carsten Müller. *Phys. Lett. B*, 696:201, 2011.
- [16] A. I. Titov, H. Takabe, B. Kämpfer, and A. Hosaka. *Phys. Rev. Lett.*, 108:240406, 2012.
- [17] T. Nousch, D. Seipt, B. Kämpfer, and A.I. Titov. *Phys. Lett. B*, 715:246, 2012.
- [18] K. Krajewska, C. Müller, and J. Z. Kamiński. *Phys. Rev. A*, 87:062107, 2013.
- [19] Martin J. A. Jansen and Carsten Müller. *Phys. Rev. A*, 88:052125, 2013.
- [20] Sven Augustin and Carsten Müller. *Phys. Lett. B*, 737:114, 2014.
- [21] A. Di Piazza, K. Z. Hatsagortsyan, and C. H. Keitel. *Phys. Rev. Lett.*, 100:010403, 2008.
- [22] S. Meuren and A. Di Piazza. *Phys. Rev. Lett.*, 107:260401, 2011.
- [23] A. Di Piazza. *Ann. Phys. (N. Y.)*, 338:302, 2013.
- [24] Victor Dinu, Tom Heinzl, Anton Ilderton, Mattias Marklund, and Greger Torgrimsson. *Phys. Rev. D*, 90:045025, 2014.
- [25] Holger Gies, Felix Karbstein, and Rashid Shaisultanov. *Phys. Rev. D*, 90:033007, 2014.
- [26] V.N. Baier, V.M. Katkov, and V.M. Strakhovenko. *Electromagnetic Processes at High Energies in Oriented Single Crystals*. World Scientific, 1998.
- [27] F. Mackenroth and A. Di Piazza. Nonlinear Double Compton Scattering in the Ultrarelativistic Quantum Regime. *Phys. Rev. Lett.*, 110:070402, Feb 2013.
- [28] A. Di Piazza, M. Tamburini, S. Meuren, and C. H. Keitel. Implementing nonlinear Compton scattering beyond the local constant field approximation. *ArXiv e-prints*, August 2017.
- [29] Vasily Yu. Kharin, Daniel Seipt, and Sergey G. Rykovanov. Higher-Dimensional Caustics in Nonlinear Compton Scattering. *Phys. Rev. Lett.*, 120:044802, Jan 2018.
- [30] Matthias Fuchs, Mariano Trigo, Jian Chen, Shambhu Ghimire, Sharon Schwartz, Michael Kozina, Mason Jiang, Thomas Henighan, Crystal Bray, Georges Ndabashimiye, et al. Anomalous nonlinear X-ray Compton scattering. *Nature Physics*, 11(11):964, 2015.
- [31] Tobias N. Wistisen. Quantum synchrotron radiation in the case of a field with finite extension. *Phys. Rev. D*, 92:045045, Aug 2015.
- [32] E. Raicher, S. Eliezer, and A. Zigler. A novel solution to the Klein-Gordon equation in the presence of a strong rotating electric field. *Physics Letters B*, 750:76 – 81, 2015.
- [33] K. K. Andersen, J. Esberg, H. Knudsen, H. D. Thomsen, U. I. Uggerhøj, P. Sona, A. Mangiarotti, T. J. Ketel, A. Dizdar, and S. Ballestrero. Experimental investigations of synchrotron radiation at the onset of the quantum regime. *Phys. Rev. D*, 86:072001, Oct 2012.
- [34] C. Bula, K. T. McDonald, E. J. Prebys, C. Bamber, S. Boege, T. Kotseroglou, A. C. Melissinos, D. D. Meyerhofer, W. Ragg, D. L. Burke, R. C. Field, G. Horton-Smith, A. C. Odian, J. E. Spencer, D. Walz, S. C. Berridge, W. M. Bugg, K. Shmakov, and A. W. Weidemann. Observation of Nonlinear Effects in Compton Scattering. *Phys. Rev. Lett.*, 76:3116–3119, Apr 1996.



- [35] M. Boca and V. Florescu. *Phys. Rev. A*, 80:053403, 2009.
- [36] Chris Harvey, Thomas Heinzl, and Anton Ilderton. *Phys. Rev. A*, 79:063407, 2009.
- [37] Thomas Heinzl and Anton Ilderton. *Opt. Commun.*, 282:1879, 2009.
- [38] F. Mackenroth, A. Di Piazza, and C. H. Keitel. *Phys. Rev. Lett.*, 105:063903, 2010.
- [39] F. Mackenroth and A. Di Piazza. *Phys. Rev. A*, 83:032106, 2011.
- [40] D. Seipt and B. Kämpfer. *Phys. Rev. A*, 83:022101, 2011.
- [41] K. Krajewska and J. Z. Kamiński. *Phys. Rev. A*, 85:062102, 2012.
- [42] D. Seipt and B. Kämpfer. *Phys. Rev. A*, 88:012127, 2013.
- [43] Victor Dinu. *Phys. Rev. A*, 87:052101, 2013.
- [44] V N Nedoreshtha, A I Voroshilo, and S P Roshchupkin. *Phys. Rev. A*, 88:052109, 2013.
- [45] K. Krajewska, M. Twardy, and J. Z. Kamiński. *Phys. Rev. A*, 89:032125, 2014.
- [46] Tobias N. Wistisen. *Phys. Rev. D*, 90:125008, 2014.
- [47] A Angioi, F Mackenroth, and A Di Piazza. *Phys. Rev. A*, 93:052102, 2016.
- [48] A Di Piazza. *Phys. Rev. A*, 95:032121, 2017.
- [49] B. King. Double compton scattering in a constant crossed field. *Phys. Rev. A*, 91:033415, Mar 2015.
- [50] A. Di Piazza. *Phys. Rev. Lett.*, 113:040402, 2014.
- [51] A. Di Piazza. *Phys. Rev. A*, 91:042118, 2015.
- [52] A. Di Piazza. *Phys. Rev. Lett.*, 117:213201, 2016.
- [53] T. Heinzl, A. Ilderton, and B. King. *Phys. Rev. D*, 94:065039, 2016.
- [54] Tom Heinzl and Anton Ilderton. *Phys. Rev. Lett.*, 118:113202, 2017.
- [55] Tom Heinzl and Anton Ilderton. *J. Phys. A: Math. Theor.*, 50:345204, 2017.
- [56] VN Baier and VM Katkov. Processes involved in the motion of high energy particles in a magnetic field. *Sov. Phys. JETP*, 26:854, 1968.
- [57] Rainer Wanzenberg. Nonlinear motion of a point charge in the 3D space charge field of a Gaussian bunch. Technical report, Dt. Elektronen-Synchrotron DESY, 2010.
- [58] Ken Takayama. Potential of a three-dimensional charge distribution powerful calculating method and its applications. Technical report, Fermi National Accelerator Laboratory (FNAL), Batavia, IL, 1982.
- [59] Vladimir B Beresteckij, Evgenij M Lifsic, and Lev P Pitaevskij. *Quantum electrodynamics*. Butterworth-Heinemann, Oxford, 2008.
- [60] Vladislav Gavrilovich Bagrov and D Gitman. *Exact solutions of relativistic wave equations*, volume 39. Springer Science & Business Media, 1990.
- [61] David J Griffiths. *Introduction to quantum mechanics*. Cambridge University Press, 2016.
- [62] N. Neitz and A. Di Piazza. Stochasticity effects in quantum radiation reaction. *Phys. Rev. Lett.*, 111:054802, Aug 2013.
- [63] T. G. Blackburn, C. P. Ridgers, J. G. Kirk, and A. R. Bell. Quantum radiation reaction in laser-electron-beam collisions. *Phys. Rev. Lett.*, 112:015001, Jan 2014.
- [64] A. Di Piazza, K. Z. Hatsagortsyan, and C. H. Keitel. Quantum radiation reaction effects in multiphoton compton scattering. *Phys. Rev. Lett.*, 105:220403, Nov 2010.
- [65] Tobias N. Wistisen, Antonino Di Piazza, Helge V. Knudsen, and Ulrik I. Uggerhøj. Experimental evidence of quantum radiation reaction in aligned crystals. *Nature Communications*, 9(1):795, February 2018.